

Study The Effect of Residual Stress on Corrosion Behaviour of Low Carbon Steel

Sarmed A. S. Altayee

College of Engineering, University of Babylon, Hilla, Iraq

Abstract: 1. Residual stress can have a significant influence on the corrosion behaviour of low-carbon steel, which is a widely used material in various industries. Low-carbon steel is widely used in industrial applications, such as construction and automotive manufacturing, due to its low cost and good mechanical properties. The primary drawback of low-carbon steel is its high corrosion sensitivity, which can lead to catastrophic failures and substantial economic losses in certain circumstances.

This study investigates the effect of residual stresses on the corrosion behaviour of low-carbon steel. According to the results of this study, it is evident that compressive residual stresses can enhance the corrosion resistance of low-carbon steel.

2. Introduction

According to (Velarde & Tinoco, 2019) Corrosion is a significant issue in the infrastructure industry, costing an estimated \$22.6 billion annually, with \$8.3 billion allocated explicitly to road bridges. Steel's inherent mechanical properties make it a preferred material for bridge construction, although corrosion remains a significant concern. The resistance of steel members in bridges may decrease over time due to corrosion-induced reductions in cross-sectional area (Jancula et al., 2019; Z. L. Li et al., 2013). Stresses that can occur during the manufacturing or fabrication process and cause residual stresses in the parts can have a substantial impact on the corrosion behaviour of steel. Previous studies have examined the relationship between corrosion and steel bridges, highlighting that Certain varieties of steel are more resistant to air corrosion, making them ideal for use in welded, riveted, or bolted structures. Nonetheless, little research has been done on how residual stresses influence the corrosion behaviour of low-carbon steel. One study investigated the effect of applied stress on the mechanical and corrosion properties of mild steel, revealing the subject's inadequate understanding (L. Li et al., 2019). Another study focused on the corrosion prevention of long-span, non-uniform continuous steel bridges and proposed methods to improve corrosion protection(Z. L. Li et al., 2013). Additionally, experimental studies on the impact of corrosion on steel bridges have been conducted, emphasising the need to consider degradation processes throughout the lifetime of an engineering construction(Jancula et al., 2019).

It has long been known that metallic components with compressive residual stresses have higher fatigue strengths. With fatigue strength enhancement as the primary objective or as a consequence of surface hardening procedures like carburising, nitriding, or physical vapour deposition, many technical components have been shot-peened or cold-worked. Other treatments, such as laser shock peening and low-plasticity burnishing, have been studied over the last decade to enhance the functionality of designed components (Dalaei et al., 2011). The

impact of thermo-mechanical treatment on the pitting corrosion of reinforcing carbon steel bars was investigated by (Barbosa et al., 2014; Štefec et al., 1979). Analysis of the steels' residual stresses revealed that the hot-rolled steels had low compressive stresses, while the cold-worked samples had substantial tensile stresses. In line with the observed internal stress distribution, hot-rolled steels exhibited somewhat better resistance to pitting corrosion than cold-worked samples (Peguet et al., 2007). This study will investigate the effect of residual stresses on the corrosion behaviour of low-carbon steel, aiming to design steel structures that are more resistant to corrosion and have a longer lifespan

3. Methodology

This research will utilize a combination of experimental and analytical methods to investigate the effect of residual stress on the corrosion behaviour of low-carbon steel .

3-1 basic corrosion:

For corrosion to occur, the formation of a corrosion cell is essential. A corrosion cell is composed of the following four key components:

- Anode: One of the two dissimilar metal electrodes in an electrolytic cell, represented as the negative terminal. The anode is the more reactive metal, where electrons are released.
- Cathode: The other electrode in the electrolytic cell is the positive terminal.
- Electrolyte: The medium that allows the flow of ions between the anode and the cathode.
- Metallic path: The conductive path that enables the movement of electrons from the anode to the cathode.

3-2 Forms of Corrosion:

Corrosion in steel structures can be classified based on three main factors: the nature of the corrosive agent, the mechanism of the corrosion process, and the visual appearance of the corroded metal. Corrosion can be categorized as wet or dry, depending on whether it requires a liquid or moisture or involves a reaction with high-temperature gases. The mechanism of corrosion can be either electrochemical or direct chemical in nature. Furthermore, corrosion can manifest as either uniform, with the metal corroding consistently across the entire surface, or localized, where only specific areas are affected. The electrochemical corrosion behaviour of the low-carbon steel specimens will then be evaluated using techniques such as potentiodynamic polarisation and electrochemical impedance(M. C. Li & Cheng, 2008).

3-3 Residual Stress Analysis:

The most important mechanisms for creating surface residual stresses are mechanical procedures, such as rolling, shot peening, and forging, which involve plastic deformation and "cold or hot working" of the material. Furthermore, residual stresses may be introduced by local yielding during other standard machining processes, such as grinding, turning, and polishing.

Nitriding and carburizing are two chemical processes that produce advantageous surface residual stress layers for ensuing service fatigue loading. On the other hand, heat treatment processes alter the metallurgical structure of the source material without altering its surface chemical composition. Induction hardening and flame hardening are the two primary heat treatment techniques that create advantageous residual stress layers. Other procedures, such as flame cutting, welding, quenching, hot rolling, and forging, can also be included in this group. Welded junctions are among the most common locations for fatigue failures caused by residual stresses, as the parent metal, weld metal, and heat-affected zone all have distinct physical properties, including varying thermal expansion coefficients. Large castings are another frequent issue associated with thermal effects and residual stresses. Although the underlying cause is yet unknown, large castings are another common problem involving thermal effects and related residual strains(Collacott, 2013; Lampman, 1996).

Metals exposed to both stress and a corrosive environment may experience stress corrosion cracking, a failure mode that forms in the surface layers and is directly related to residual stresses. Materials that experience loads more significant than their yield point undergo permanent deformation, which does not entirely disappear when the load is removed. When beams undergo moments that cause partial plasticity in bending applications, some of the beam sections stay elastic while the outer fibres yield. When the load is removed, the elastically strained portions of the material cannot return to their initial unstressed state because of the permanent deformation in the yielding sections (figure 3-1). As a result, the material experiences residual strains. It is frequently assumed that the unloading process, whether from partially or totally plastic states, occurs in a purely elastic manner in order to measure the size of these residual stresses. Techniques like hole drilling, neutron diffraction, and X-ray diffraction can be used to assess these residual stresses.(Lampman, 1996)

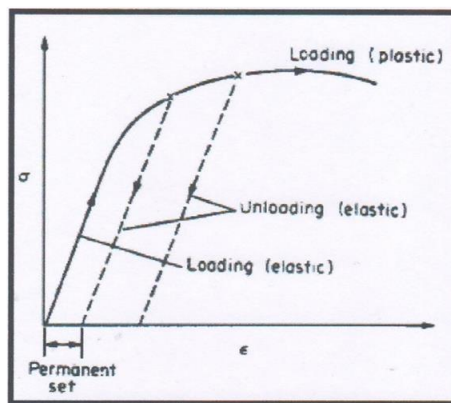


Fig 3-1 Tensile test stress-strain curve showing elastic unloading process from any load condition

4. Experimental Work

In this study, four specimens were used to investigate the effect of residual stresses on corrosion of low-carbon steel.

4-1 materials:

The materials used in this study were low-carbon steel. The specimens were prepared through a series of manufacturing processes to induce different types of residual stresses.

Table 4-1 Micro alloy low carbon steel is used by chemical composition (wt %):

Steel composition	C %	Si %	Mn %	P %	S %	Cr%	Ni %	Ma %
Element percentage	< 0.2	0.26	< 0.9	0.01	0.03	<1.3	0.11	0/01

4-2 Test specimens:

In this investigation, four specimens were analysed. The specimens utilised in the experiment have the following measurements: length = 9 cm, width = 0.9 cm, and thickness = 0.2 cm. The specimens' shapes are shown in figures (4-1) and (4-2).



Fig 4-1 Specimens before the mechanical polishing

Fig 4-2 Specimens after the mechanical polishing

4-3 Specimen Preparation:

To find out how residual stresses affect corrosion, four specimens were analysed:

- Specimen one was heated in an oven and slowly cooled to remove any residual stresses.
- Specimen two was subjected to a compressive load to introduce compressive residual stress.
- Specimen three was subjected to a bending load to introduce bending residual stress.
- Specimen four was subjected to thermal treatment by rapid quenching in water after heating.

4-3 corrosion test:

The polarization technique (as shown in Figure 4-3) was used to study the corrosion behaviour of low-alloy low-carbon steel specimens in a 3% NaCl solution at room temperature. Polarization tests were conducted in a three-electrode system using a digital multimeter.

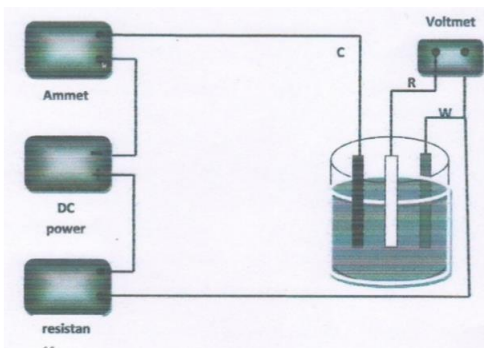


Fig 4-3 Polarization test

The test specimen was the working electrode, a saturated calomel electrode was the reference electrode, and a graphite electrode was the counter electrode. The 3% NaCl solution acted as the electrolyte. The reference and graphite electrodes were only used during potential measurements and were removed afterwards. Tafel lines were constructed over 15 days to determine the corrosion current and potential. The corrosion rate was determined by measuring the I_{corr} . After the corrosion test, the specimens were cleaned.

5. Results and Discussion

Table 5-1 provides a summary of the corrosion test findings for the four specimens.

Table 5-1 I_{corr} of the four specimens

Applied load	I_{corr} at 0 day	I_{corr} at 4 days	I_{corr} at 7 days	I_{corr} at 15 days
Without any load	0.009	0.007	0.02	0.019
Under compression	0.0068	0.014	0.011	0.016
Under bending	0.01	0.0175	0.011	0.0195
Under thermal treatment	0.01	0.012	0.013	0.0125

When compared to the other specimens, the specimen with compressive residual stresses exhibited superior corrosion resistance compared to the specimen without any load and the one which is under bending; however, the specimen subjected to thermal treatment shows good resistance to corrosion, as indicated by the results.

5-1 Polarization curves without stress:

Figures (5-1) to (5-4) show the polarization curves for the specimen without stress tested directly after 4 days, after 7 days and after 15 days.

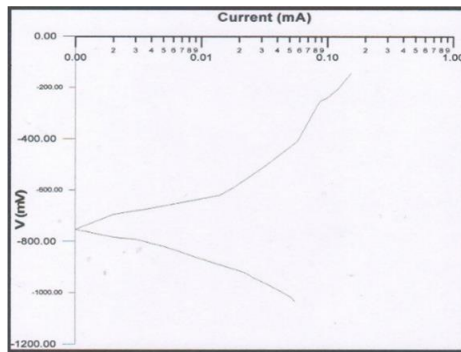


Fig 5-1 Sample number (1) in (0) Day

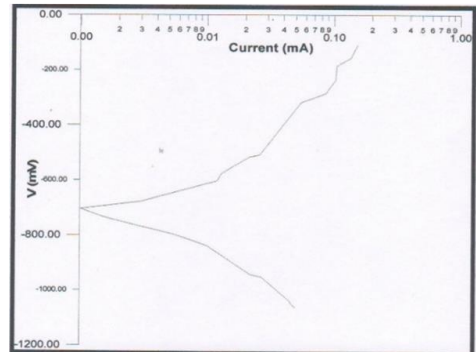


Fig 5-2 Sample number (1) in (4) Days

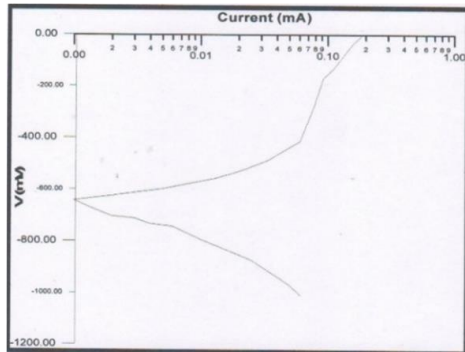


Fig 5-2 Sample number (1) in (7) Days

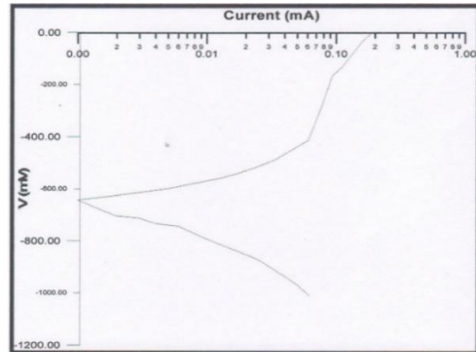


Fig 5-2 Sample number (1) in (15) Days

Figures (5-4) to (5-8) show the polarization curves for the specimen with compressive residual stress tested directly after 4 days, after 7 days and after 15 days.

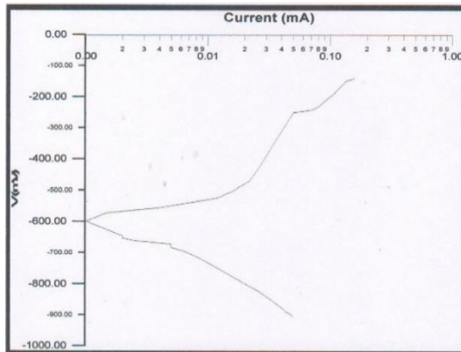


Fig 5-5 Sample number (2) in (0) Day

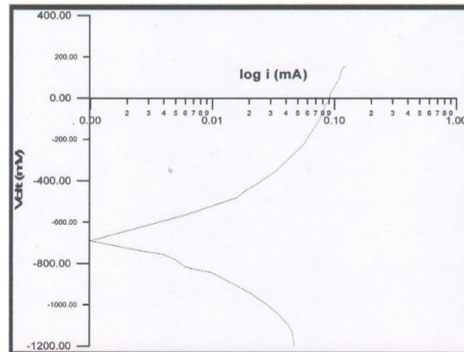


Fig 5-6 Sample number (2) in (4) Days

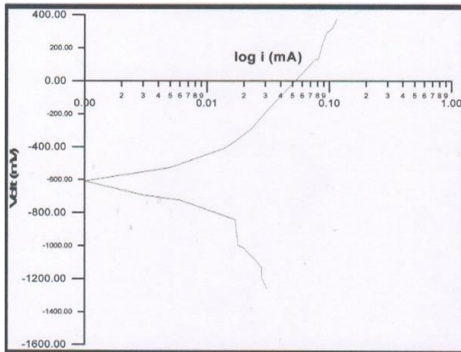


Fig 5-7 Sample number (2) in (7) Days

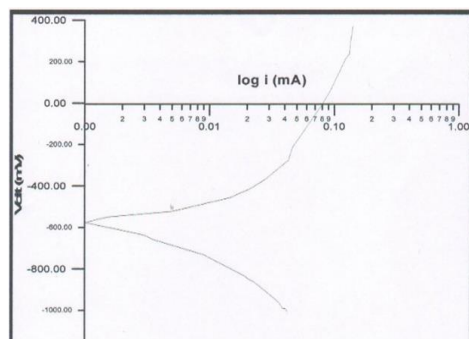


Fig 5-8 Sample number (2) in (15) Days

Figures (5-9) to (5-12) show the polarization curves for the specimen subjected to bending stress tested directly after 4 days, after 7 days and after 15 days.

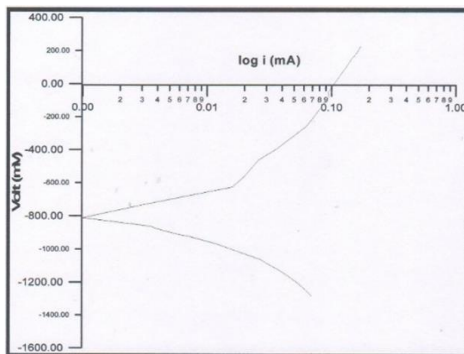


Fig 5-9 Sample number (3) in (0) Day

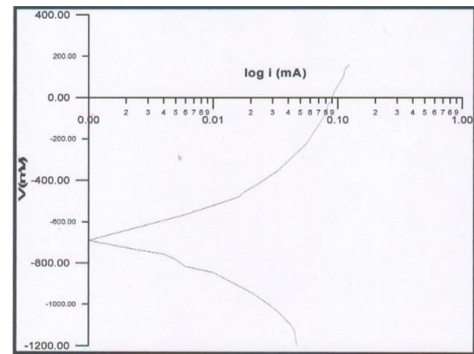


Fig 5-10 Sample number (3) in (4) Days

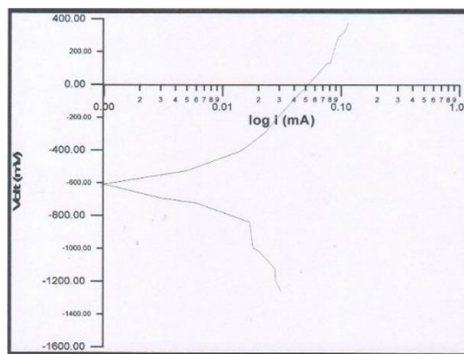


Fig 5-11 Sample number (3) in (7) Days

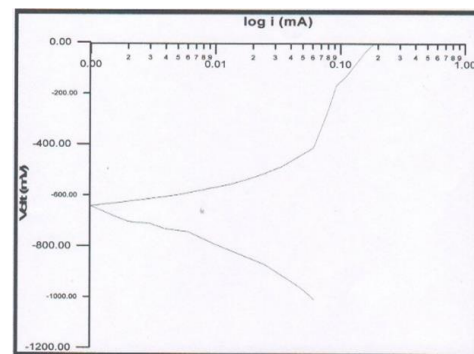


Fig 5-12 Sample number (3) in (15) Days

Figures (5-12) to (5-16) show the polarization curves for the specimen subjected to thermal treatment & quenching, tested directly after 4 days, after 7 days and after 15 days.

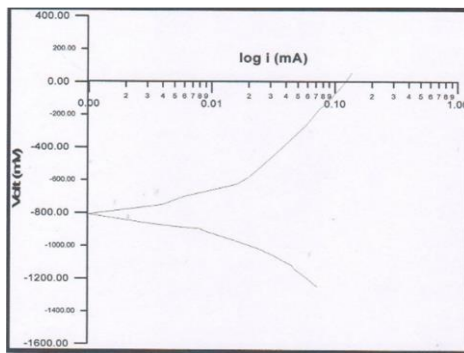


Fig 5-13 Sample number (4) in (0) Day

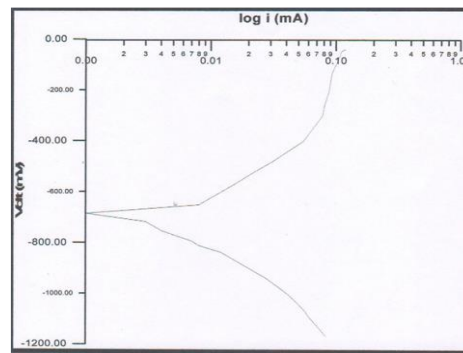


Fig 5-14 Sample number (4) in (4) Days

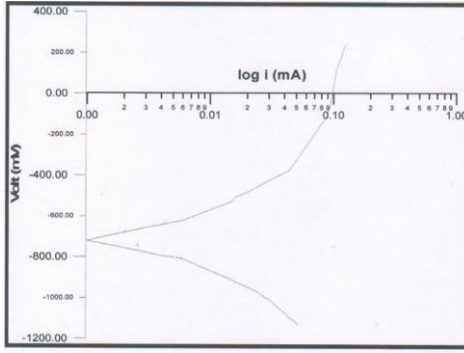


Fig 5-15 Sample number (4) in (7) Days

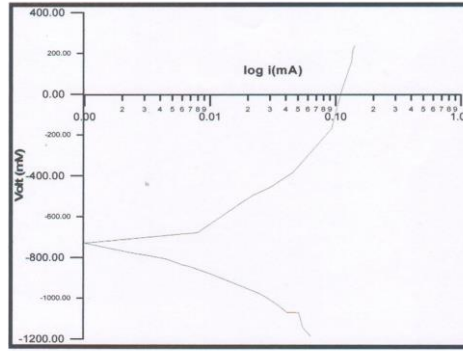


Fig 5-16 Sample number (4) in (15) Days

Figures (5-17) to (5-20) show the polarization curves for the four specimens tested directly after 4 days, after 7 days and after 15 days.

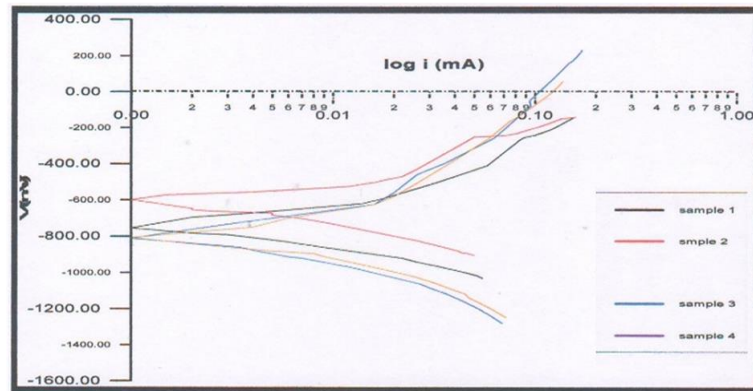


Fig 5-17 Curves of the four samples at (0) day

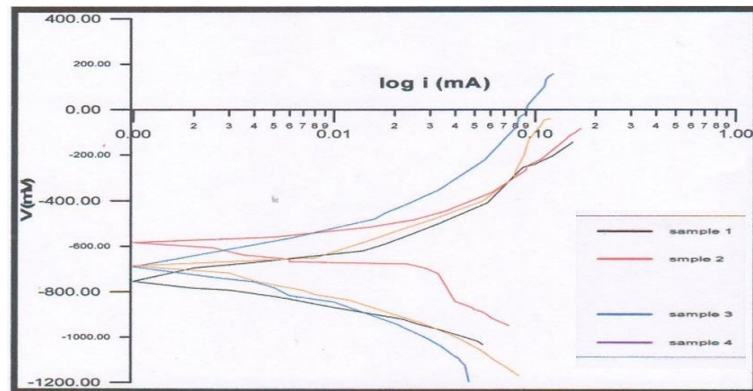


Fig 5-18 Curves of the four samples at (4)

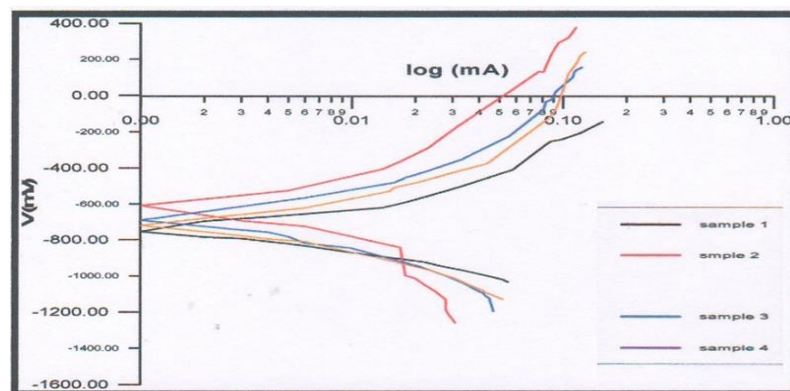


Fig 5-19 Curves of the four samples at (7)

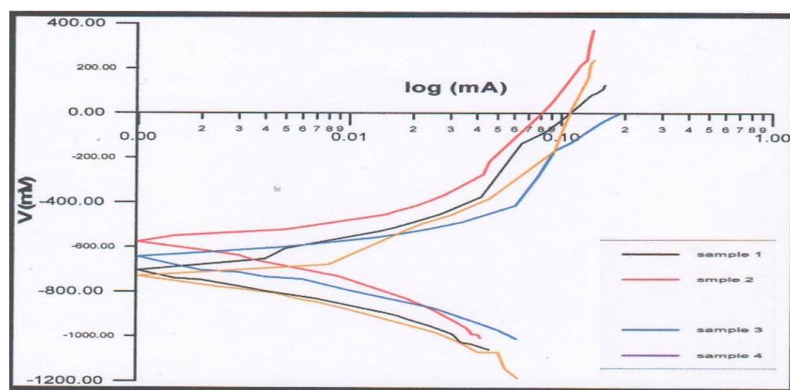


Fig 5-20 Curves of the four samples at (15) days

5-2 Corrosion Rate:

The following formula is used to calculate the corrosion rate:

$$\text{Corrosion rate (mpy)} = 0.129 \times (I_{\text{corr}}/zF)$$

where

I_{corr} is the corrosion current mA / cm²

z is the number of electrons transferred per metal atom

F is the Faraday number $\approx 96,485$ C/mol

Area of the sample is 20.16 (cm²)

The corrosion rate was calculated from the weight loss measurement.

Table 5-2. The corrosion rate result.

Specimen type	Corrosion rate (0 days)	Corrosion rate (4 days)	Corrosion rate (7 days)	Corrosion rate (15 days)
Subjected to residual stress removal treatment	2.891×10^{-7}	2.319×10^{-7}	6.63×10^{-7}	6.296×10^{-7}
Subjected to compression load	2.252×10^{-7}	4.638×10^{-7}	3.642×10^{-7}	5.3×10^{-7}
Subjected to a bending load	3.315×10^{-7}	5.801×10^{-7}	3.642×10^{-7}	6.463×10^{-7}
Subjected to heading and quenching	3.315×10^{-7}	3.97×10^{-7}	4.304×10^{-7}	4.194×10^{-7}

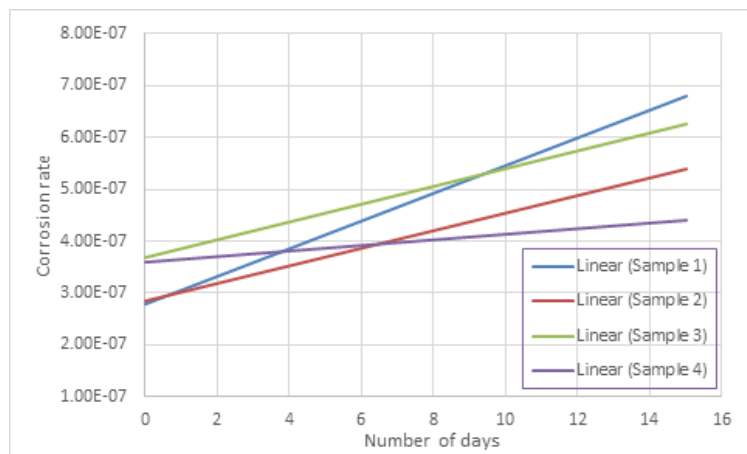


Fig 5-21 Corrosion rate of the four samples

Dissection

The plots of I_{corr} for the four samples, against exposure time to salt solution, are displayed in Figures 5-17 to 5-20. For the four samples previously described, Figure 5-21 illustrates the relationship between the corrosion rate (mpy) and the exposure duration to the 3% NaCl salt solution. The results shown in Figure 5-21 indicate that the residual stress in the low-carbon steel specimens has a significant influence on their corrosion behaviour. The specimen with compressive residual stresses exhibited better corrosion resistance, with the lowest corrosion rate when compared to specimens one and three. This can be attributed to the fact that compressive residual stresses inhibit the initiation and propagation of corrosion pits on the steel surface (Chen et al., 2013). The compressive stresses counteract the tensile stresses that can develop during corrosion, thereby preventing the formation of cracks. The specimen subjected to thermal treatment from rapid quenching showed a low and stable corrosion rate compared with other samples due to the formation of dual-phase steel and its refined grain structure. The ferrite phase in the dual phase steel is more electrochemically active (anodic) than the martensitic phase

(cathodic), leading to micro galvanic coupling. This can cause preferential corrosion of the ferrite phase when exposed to aggressive environments like acidic solutions.

These findings are consistent with the observations reported in the literature(Fang et al., 2004; Malumbela et al., 2009; Mansoor & Zhang, 2013; Moreno et al., 2014). The composition, structure, and morphology of the surface film on steel play a crucial role in controlling the corrosion rate, which is influenced by the residual stresses (Yohai et al., 2013). Overall, the results demonstrate the importance of considering the residual stresses when evaluating the corrosion performance of low-carbon steel components.

6. Conclusions

Samples subjected to a compression load corrode at a corrosion rate lower than those without mechanical load, due to the fact that compression stress decreases stress corrosion, while tensile stress increases stress corrosion. Corrosion of the sample that is heat-treated to produce dual-phase steel starts with a corrosion rate higher than that of the sample not subjected to any load and the one with compressive residual stresses, but after a few days, it corrodes at a rate less than that of the other samples due to the microstructure of the dual phase steel and due to the unique corrosion behaviour of dual-phase martensitic steel.

7. Reference

1. Barbosa, B. A. R. S., Tavares, S. S. M., Bastos, I. N., Silva, M. R., & De Macedo, M. C. S. (2014). Influence of heat treatments on microstructure and pitting corrosion resistance of 15%Cr supermartensitic stainless steel. *Corrosion Engineering Science and Technology*, 49(4), 311–315. <https://doi.org/10.1179/1743278214Y.0000000156>
2. Chen, Y. H., Chen, M. J., Sun, L. Y., & Wang, X. M. (2013). Fatigue stiffness analysis of corroded RC beams. *Applied Mechanics and Materials*, 351–352, 450–453. <https://doi.org/10.4028/www.scientific.net/AMM.351-352.450>
3. Collacott, R. A. (2013). Residual Stresses. *Chartered Mechanical Engineer*, 26(8), 45–47. <https://doi.org/10.31399/ASM.TB.UHCF3.T53630035>
4. Dalaei, K., Karlsson, B., & Svensson, L. E. (2011). Stability of shot peening induced residual stresses and their influence on fatigue lifetime. *Materials Science and Engineering: A*, 528(3), 1008–1015. <https://doi.org/10.1016/j.msea.2010.09.050>
5. Fang, C., Kou, X., Chen, L., Chen, B., & Zhu, C. (2004). Experimental study of the effect of reinforcement corrosion on bond strength. *Key Engineering Materials*, 274–276(I), 1041–1046. <https://doi.org/10.4028/www.scientific.net/KEM.274-276.1041>
6. Jancula, M., Vican, J., & Spiewak, A. (2019). Experimental Research of Corrosion Effects on Steel Bridges. *IOP Conference Series: Materials Science and Engineering*, 661(1). <https://doi.org/10.1088/1757-899X/661/1/012138>
7. Lampman, S. R. (1996). ASM Handbook: Volume 19, Fatigue and Fracture. *ASM International*, 19(9), 557–565. https://www.asminternational.org/results/-/journal_content/56/25656855/PUBLICATION/
8. Li, L., Li, C.-Q., & Mahmoodian, M. (2019). Effect of Applied Stress on Corrosion and Mechanical Properties of Mild Steel. *Journal of Materials in Civil Engineering*, 31(2). [https://doi.org/10.1061/\(ASCE\)MT.1943-5533.0002594](https://doi.org/10.1061/(ASCE)MT.1943-5533.0002594)
9. Li, M. C., & Cheng, Y. F. (2008). Corrosion of the stressed pipe steel in carbonate–bicarbonate solution studied by scanning localized electrochemical impedance spectroscopy. *Electrochimica Acta*, 53(6), 2831–2836. <https://doi.org/10.1016/j.electacta.2007.10.077>

10. Li, Z. L., Ding, H. Y., Du, Y., & Xue, J. (2013). The corrosion prevention research of Long-span non-uniform continuous steel bridges. *Applied Mechanics and Materials*, 361–363, 1129–1132. <https://doi.org/10.4028/WWW.SCIENTIFIC.NET/AMM.361-363.1129>
11. Malumbela, G., Moyo, P., & Alexander, M. (2009). Behaviour of RC beams corroded under sustained service loads. *Construction and Building Materials*, 23(11), 3346–3351. <https://doi.org/10.1016/J.CONBUILDMAT.2009.06.005>
12. Mansoor, Y. A., & Zhang, Z. Q. (2013). The reinforcement bond strength behavior under different corrosion condition. *Research Journal of Applied Sciences, Engineering and Technology*, 5(7), 2346–2353. <https://doi.org/10.19026/RJASSET.5.4663>
13. Moreno, E., Cobo, A., Palomo, G., & González, M. N. (2014). Mathematical models to predict the mechanical behavior of reinforcements depending on their degree of corrosion and the diameter of the rebars. *Construction and Building Materials*, 61, 156–163. <https://doi.org/10.1016/J.CONBUILDMAT.2014.03.003>
14. Peguet, L., Malki, B., & Baroux, B. (2007). Influence of cold working on the pitting corrosion resistance of stainless steels. *Corrosion Science*, 49(4), 1933–1948. <https://doi.org/10.1016/J.CORSCI.2006.08.021>
15. Štefec, R., Franz, F., & Holeček, A. (1979). Effect of Heat Treatment on Pitting Corrosion of austenitic Cr-Ni-Mo steels in sodium chloride solution. *Materials and Corrosion*, 30(3), 189–197. <https://doi.org/10.1002/MACO.19790300305>
16. Velarde, P. A. H., & Tinoco, M. A. P. (2019). Main Advantages of Steel in Bridges Construction using improved corrosion. *International Journal of Advanced Engineering Research and Science*, 6(11), 323–327. <https://doi.org/10.22161/IJAERS.611.50>
17. Yohai, L., Vázquez, M., & Valcarce, M. B. (2013). Phosphate ions as corrosion inhibitors for reinforcement steel in chloride-rich environments. *Electrochimica Acta*, 102, 88–96. <https://doi.org/10.1016/J.ELECTACTA.2013.03.180>